

Plasma deposition of thiophene derivatives under atmospheric pressure

Peer-reviewed author version

DAMS, Roel; VANGENEUGDEN, Dirk & VANDERZANDE, Dirk (2006) Plasma deposition of thiophene derivatives under atmospheric pressure. In: CHEMICAL VAPOR DEPOSITION, 12(12). p. 719-727.

DOI: 10.1002/cvde.200606483

Handle: <http://hdl.handle.net/1942/1459>

# **Plasma Deposition of Thiophene Derivatives at Atmospheric Pressure**

***Roel Dams<sup>\*</sup>, Dirk Vangeneugden<sup>\*</sup>, and Dirk Vanderzande***

**\*Mr. Dams R., Dr. D. Vangeneugden**

**VITO, Flemish Institute for Technological Research**

**Boeretang 200, B-2400 Mol, Belgium**

**E-mail: [Roel.Dams@vito.be](mailto:Roel.Dams@vito.be)**

**Tel: ++32 14 33 57 31**

**E-mail: [Dirk.Vangeneugden@vito.be](mailto:Dirk.Vangeneugden@vito.be)**

**Tel: ++32 14 33 56 20**

**Fax: ++32 14 32 11 86**

**Prof. Dr. D. Vanderzande**

**University of Hasselt, Institute for Material Research (IMO), Division Chemistry**

**Agoralaan, Building D, B-3590 Diepenbeek, Belgium**

## **ABSTRACT**

Plasma deposition of conjugated polymer films at atmospheric pressure is described. The thiophene derivatives, thiophene, 3-methylthiophene and 3,4-ethylenedioxythiophene were used as monomers. The plasma depositions with the different precursors were compared with analytical techniques such as XPS, FT-IR, UV-VIS and resistance measurements. Good results were obtained with pulsed plasma depositions of poly(3,4-ethylenedioxythiophene). Conductivities up to  $1 \times 10^{-2}$  S/cm were measured.

Keywords: plasma, atmospheric pressure, conjugated polymer, conducting polymer, thiophene

## 1. Introduction

In general, organic polymers are known to be electrical insulators. However, since the revolutionary discovery of conductivity in doped polyacetylene in 1977 by the groups of Alan J. Heeger, Alan G. MacDiarmid and Hideki Shirakawa<sup>[1]</sup> (Nobel Prize in chemistry, 2000), a new group of polymers i.e. conjugated polymers, was born. Nowadays, conjugated polymers are the subject of numerous investigations towards their applicability in polymeric LEDs<sup>[2-3]</sup>, organic thin film transistors (OTFTs)<sup>[4]</sup>, photo detectors<sup>[5]</sup>, (bio)sensors<sup>[6]</sup>, hybrid and/or all organic solar cells and photovoltaics<sup>[7]</sup>, corrosion inhibiting coatings<sup>[8]</sup> and antistatic layers. The main advantages for applying conjugated polymers are the production of large-area applications, film flexibility and reduced production cost.

Chemical and electrochemical synthesis of conjugated polymer coatings is well described in literature<sup>[9-10]</sup>. However, both methods have their drawbacks. In general, the typical structure with alternate single and double bonds leads to rigid, insoluble polymers. Processing of the polymers, resulting from chemical polymerization is therefore difficult. If the substrate is conductive, this problem can be solved by using electropolymerization with deposition directly on the substrate. Nevertheless, both chemical and electrochemical synthesis, are usually performed in batch processes. This is the reason why, until today, they are only used for small scale applications with high added values. High speed, in-line processing, with low production cost, is not yet possible.

Recently, synthesis of thin polymer films by use of plasma polymerization has emerged as an interesting new approach. Plasma polymerization is a 'dry' technique that doesn't require the use of solvents. From an ecological and economical point of view, the absence of solvents and solvent waste offers a lot of advantages. At first, plasma polymerization was used for the formation of thin passive layers but it has recently found its way towards other applications. Some of those applications incorporate the deposition of conjugated polymers.

Plasma polymerizations of thiophene and derivatives at low pressure have already been reported<sup>[11-27]</sup>. However, since this technique requires a high vacuum, it can only be done in a batch process. For continuous processing, polymerization should be done in a plasma reactor that can work at atmospheric pressure.

In this paper, plasma polymerization of thiophene derivatives at atmospheric pressure is described. Besides the possibility of in-line processing, plasma polymerization at atmospheric pressure has some other advantages over deposition at low pressure. Since the chance that a gas molecule collides with another is higher at atmospheric pressure than in vacuum, energy transfer is more efficient. At vacuum pressure, the monomer molecules are often fragmented, because the plasma species are highly energetic. The lower energy of plasma species at atmospheric pressure results in a better retention of the chemical structure. This theory is confirmed by Groenewoud et al.<sup>[27]</sup>, who demonstrated that, even with a small pressure increase (from 0.06 mbar to 0.3 mbar), fragmentation of thiophene can be decreased.

This article reports the possibility to deposit conjugated polymer coatings from thiophene derivatives with a plasma reactor, working at atmospheric pressure. Coatings deposited from thiophene, 3-methylthiophene and 3,4-ethylenedioxythiophene, are compared. A detailed characterization is done with the help of conventional techniques such as FT-IR, UV/VIS and XPS.

## **2. Results and Discussion**

### **2.1. Synthesis**

Plasma polymerization at atmospheric pressure of three different thiophene derivatives (Figure 1) is demonstrated. The monomers used, are thiophene (Th), 3-methylthiophene (3MeTh) and 3,4-ethylenedioxythiophene (EDOT). The reaction conditions are presented in

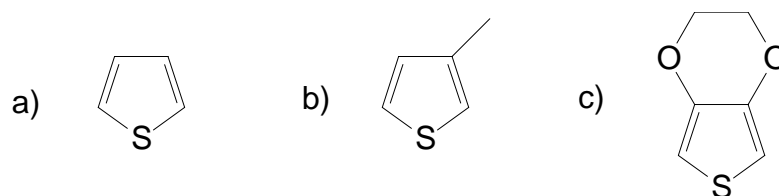


Figure 1: Structure of three thiophene derivatives: (a) thiophene (Th); (b) 3-methylthiophene (3MeTh); (c) 3,4-ethylenedioxythiophene (EDOT).

Table 1. Plasma conditions during polymerization of thiophene, 3-methylthiophene and EDOT at atmospheric pressure.

N°	Monomer	Power (W/cm <sup>2</sup> )	Gas flow (l/min) <sup>[a]</sup>	% Oxygen	Reaction mode <sup>[b]</sup>
1	Th	0.27	23	0	Continuous
2	Th	0.27	23	0.7	Continuous
3	3MeTh	0.27	23	0	Continuous
4	3MeTh	0.27	23	0.7	Continuous
5	EDOT	0.36	13	1.2	Pulsed

[a] The carrier gas is nitrogen in all experiments.

[b] EDOT is polymerized in a block wave pulsed mode with a 10s wave length. This means that the power is switched on for 5s and switched off for another 5s.

table 1. The monomers thiophene and 3-methylthiophene polymerize easily in an atmospheric pressure plasma. As shown in table 2, the deposition rate in a nitrogen plasma is quite high. When a small amount of oxygen (<1%) is added to the carrier gas, the

deposition rate increases even more. When polymerized in traditional wet chemical techniques, thiophene derivatives polymerize following an oxidative condensation mechanism. The addition of oxygen to the plasma discharge, results in the formation of strongly oxidizing species like oxygen radicals and ozone. Since this fastens the plasma polymerization, the reaction mechanism for plasma deposition is probably also oxidative. All the polymerizations done with thiophene, as well as with 3-methylthiophene result in yellow brown coatings. This colour differs significantly from the polymers synthesized with the traditional techniques (both polythiophene and poly(3-methylthiophene) have a red colour in their undoped state).

Table 2. Deposition rate of plasma polymerized thiophene derivatives

N°	Monomer	Oxygen <sup>[a]</sup>	Position <sup>[b]</sup> (cm)	Deposition rate (nm/min)
<b>1</b>	Th	-	5	220
<b>2</b>	Th	+	5	330
<b>3</b>	3MeTh	-	5	210
<b>4</b>	3MeTh	+	5	260
<b>5a</b>	EDOT	+	5	70
<b>5b</b>	EDOT	+	10	20

[a] (+) Oxygen is present in the carrier gas; (-) No oxygen in the carrier gas.

[b] The position of the sample on the electrode is presented as the distance from the gas inlet.

It's more difficult to obtain a plasma coating at atmospheric pressure with the EDOT monomer (table 1). To obtain a coating with this monomer, a small amount of oxygen is

necessary. Furthermore, the reaction must occur in a pulsed power mode. This means that the power is repeatedly switched on for 5s and then switched off for another 5s, during plasma polymerization. Table 2 shows that the deposition rate with this technique depends on the distance from the gas inlet. Close to the gas inlet deposition is three times faster than at a distance of 10 cm. The colour is also different in these two plasma regions. Close to the gas inlet, the colour is green-blue, while at a larger distance, a blue colour can be observed. A possible explanation for this phenomenon can be found in concentration differences. When plasma deposition is done in a continuous mode, a brown coating is formed close to the gas inlet. Further away from the gas inlet, there is no deposition at all. This means that plasma deposition is fast, close to the gas inlet, where the concentration is highest. At a larger distance, monomer concentration is too far reduced to form the polymer. The brown colour indicates that the so formed polymer differs from the one polymerized with traditional techniques. The monomer appears to be (partially) fragmented. When the on/off pulsed mode is used, the situation is different. During the first plasma off time, the plasma reactor is filled with the monomer, but with a concentration gradient. During the on time, polymer deposition (of the brown polymer) starts, but with high deposition rate close to the gas inlet where monomer concentration is high and slow deposition rate further away from the gas inlet where monomer concentration is low. When the plasma is turned off again, new monomer is mixed with the active species that are still present in the reactor. These active species start polymerization in less severe conditions, with formation of the actual blue polymer. This polymerization reaction occurs at the complete surface of the electrode. During the off time, the concentration gradient is also established again, which makes the cycle complete.

The nice results, obtained with the pulsed plasma polymerization of the EDOT monomer, suggest that pulsing could also be interesting for the plasma polymerization of thiophene



and 3-methylthiophene. However, pulsed plasma depositions with these monomers still resulted in brown-yellow coatings. Probably, there is no polymerization during the plasma off times.

## 2.2. Composition

The atomic composition of the plasma deposited coatings is studied with XPS spectroscopy. The results are shown in table 3. For the plasma depositions with thiophene (1-2), the expected structural formula is  $C_4S$ . This carbon/sulphur ratio can indeed be calculated with XPS. It is a little bit higher because of the elimination of some sulphur compounds. Remarkable is that even when there is no oxygen added to the carrier gas, a quite high oxygen concentration can be found in the resulting coating. This can be explained by both oxygen traces in the plasma reactor and by reaction with air after the reactor is opened. Since XPS spectroscopy only measures the composition of the surface of the coating, one can expect that reaction with surrounding air after plasma polymerization might be an important reason for the high oxygen concentration. Oxygen concentration in the bulk of the coating might be lower. As expected, the oxygen concentration increases when oxygen is added to the carrier gas. Both depositions with thiophene contain a small amount of nitrogen, resulting from reaction with the carrier gas.

Table 3. Atomic composition of plasma polymerized thiophene derivatives, measured by XPS spectroscopy.

N°	Monomer	Oxygen <sup>[a]</sup>	Position <sup>[b]</sup> (cm)	%S	%C	%O	%N	Formula
1	Th	-	5	15	66	16	3	$C_{4,4}SO_{1,1}N_{0,2}$
2	Th	+	5	15	63	20	2	$C_{4,2}SO_{1,3}N_{0,1}$

<b>3</b>	<b>3MeTh</b>	-	<b>5</b>	15	72	9	4	$C_{4,8}SO_{0,6}N_{0,3}$
<b>4</b>	<b>3MeTh</b>	+	<b>5</b>	13	67	17	3	$C_{5,2}SO_{1,3}N_{0,2}$
<b>5a</b>	<b>EDOT</b>	+	<b>5</b>	8	60	30	2	$C_{7,5}SO_{3,8}N_{0,3}$
<b>5b</b>	<b>EDOT</b>	+	<b>10</b>	9	58	31	2	$C_{6,4}SO_{3,4}N_{0,2}$

---

[a] (+) Oxygen is present in the carrier gas; (-) No oxygen in the carrier gas.

[b] The position of the sample on the electrode is presented as the distance from the gas inlet.

Plasma deposition with 3-methylthiophene (3-4) is expected to result in polymer coatings with structural formula  $C_5S$ . XPS measurements show that the expected carbon/sulphur ratio can indeed be found in the plasma coating. When no oxygen is added to the carrier gas, the oxygen concentration is lower, compared to the deposition with thiophene (1). Apparently the methyl group in the 3-position delays the reaction with oxygen. Again, one must keep in mind that this concentration is measured at the surface of the coating and that oxygen concentration in the bulk might be lower. Addition of oxygen to the carrier gas with formation of ozone and oxygen radicals, results in an increase of the oxygen amount in the coating. A small amount of nitrogen is also built in by reaction with the carrier gas.

Plasma deposition with EDOT is expected to result in coatings with structural formula  $C_6O_2S$ . Table 3 shows that the results are different for the coating deposited close to the gas inlet (5a) and the coating deposited at a distance of 10 cm from the gas inlet (5b). Close to the gas inlet, the carbon concentration in the coating is higher than expected. This is due to the elimination of sulphur compounds. Further away from the gas inlet, the carbon/sulphur ratio is respected better. Also the oxygen concentration is higher than the expected value in both depositions. The addition of oxygen to the carrier gas results in the formation of some additional oxygen functionalities in the plasma deposited coating. Although the carrier gas

mainly exists out of nitrogen gas, only a small amount of nitrogen is found in the plasma coatings.

In conclusion can be stated that plasma depositions with thiophene, 3-methylthiophene and EDOT can be done with good retention of the carbon/sulphur ratio of the monomer. The carrier gas, containing nitrogen and oxygen, is also built into the plasma coatings.

### **2.3. Chemical Structure**

Chemical structure of the samples is studied with infrared spectroscopy. The FT-IR spectra are shown in figures 2,3 and 4. Figure 2 presents the infrared spectra of the plasma polymerized polythiophene synthesized in a nitrogen plasma (A) and a nitrogen/oxygen plasma (B). These spectra are compared with the spectrum of the original monomer (C). A detailed peak assignment is presented in table 4. Both spectra, (A) and (B) show peaks around  $1410\text{ cm}^{-1}$ , and  $600\text{ cm}^{-1}$ , which can be characterized by the C=C stretch in the aromatic 5-ring and the ring vibration respectively. This means that at least a part of the original monomer structure is still present in the final coating. Note that the frequency, position and the number of these peaks is influenced by the conjugation length, morphology and doping state of the conjugated polymers. Differences between the two polymer spectra and between polymer and monomer spectra are thus expected. Both spectra, also show an absorption peak around  $3030\text{ cm}^{-1}$ , which comes from the C-H stretching vibration on position 3 and 4 of the thiophene ring. This proves that the plasma polymerized coating still contains double bonds. Around  $3100\text{ cm}^{-1}$ , the C-H stretch on the 2 and 5 position of the thiophene ring can be seen. One should expect that when polymerization occurs in a traditional way, this absorption is no longer present in the polymer spectrum, since polymerization occurs in the 2 and 5 position. Plasma polymerization thus results in low molecular weight polymers that are highly branched (polymerization in 3 and 4 position

instead of 2 and 5). Certain absorptions in the infrared region that are not present in the monomer spectrum suggest fragmentation of the monomer structure. Evidence for saturated carbons can be found in the C-H stretching vibrations around  $2900\text{ cm}^{-1}$ . Around  $2200\text{ cm}^{-1}$ , the C-C alkyne stretching vibration can be seen. The presence of an alkyne C-H stretching vibration around  $3300\text{ cm}^{-1}$  shows that this alkyne function is situated at the end of the polymer chains. It seems that the polymerization reaction doesn't continue at the place where the alkyne function is formed. Although no oxygen is added, when the monomer is polymerized in a nitrogen plasma, the infrared spectrum (figure 2A) still shows the presence of some absorption bands around  $1650\text{ cm}^{-1}$ , which is typical for carbonyl functions. This might be due to the oxygen traces in the carrier gas or reactor. Oxygen forms ozone and oxygen radicals in the plasma, which have the ability to break double bonds with the formation of ketones (or aldehydes). Three types of ketones can be found in the spectrum. The one at  $1715\text{ cm}^{-1}$  is typical for saturated ketones. When the ketone function is  $\alpha,\beta$ -unsaturated, its absorption frequency decreases ( $1666\text{ cm}^{-1}$ ). The lowest carbonyl stretching frequency at  $1634\text{ cm}^{-1}$ , might be due to a ketone function with a more extended conjugation or one that has a decreased frequency because of hydrogen bonding (e.g. enolized 1,3-diketone). When oxygen is added to the carrier gas (figure 2B), the plasma consists of an even higher ozone concentration. This results in stronger carbonyl absorptions around  $1650\text{ cm}^{-1}$ . The carbonyl functions that appear in these plasma polymerized polythiophene coatings make the coating very hydrophilic. As a result water from the surrounding air is easily absorbed, which is the reason for the strong (water) O-H stretching bands around  $3400\text{ cm}^{-1}$  that appear in all the spectra.

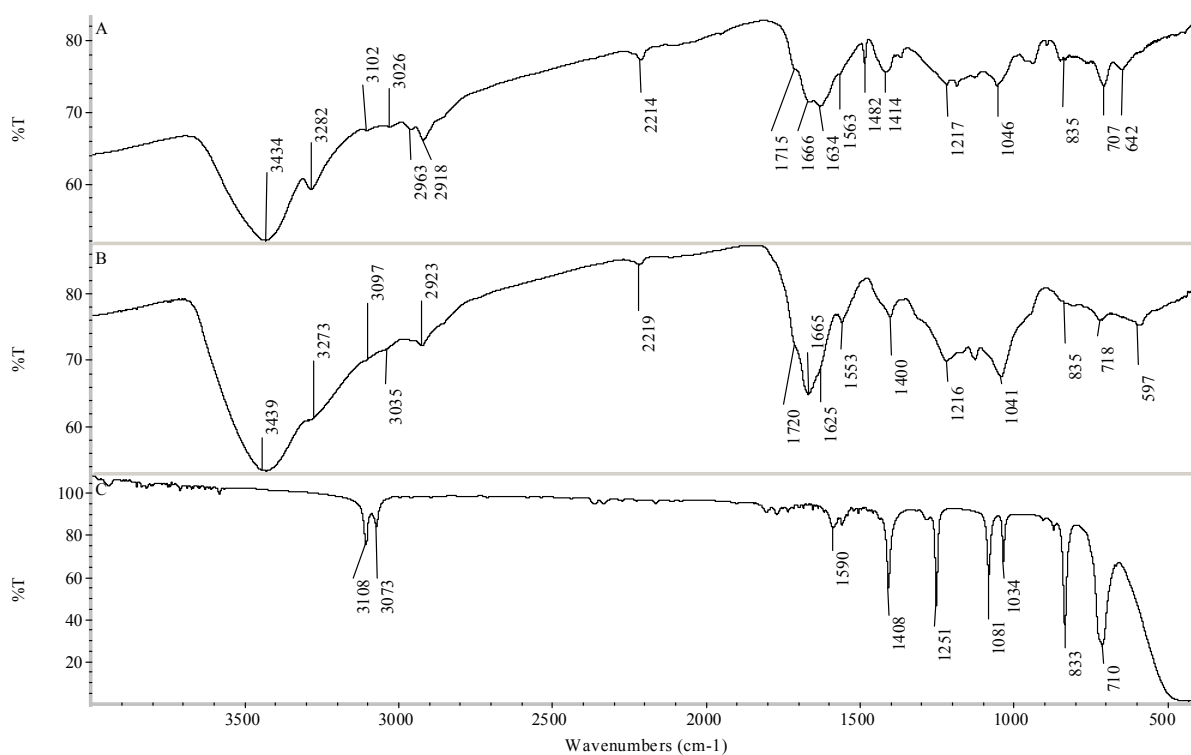


Figure 2: Infrared spectra of (A) polythiophene plasma polymerized in nitrogen gas, (B) polythiophene plasma polymerized in a nitrogen/oxygen mixture, (C) the monomer thiophene.

Table 4: Detailed infrared peak assignment of (A) polythiophene plasma polymerized in nitrogen (B) polythiophene plasma polymerized in a nitrogen/oxygen mixture (C) the monomer thiophene.

Vibration	A (cm <sup>-1</sup> )	B (cm <sup>-1</sup> )	C (cm <sup>-1</sup> )
<b>O-H</b> stretch	3434	3439	-
<b>C≡C-H</b> stretch	3282	3273	-
<b>C=C-H</b> stretch	3026+3102	3035+3097	3073+3108
<b>C-C-H</b> stretch	2918+2963	2923	-
<b>C≡C</b> stretch	2214	2219	-
<b>C=O</b> stretch	1634+1666+1715	1625+1665+1720	-

<b>C=C stretch</b>	1414+1482+1563	1400+1553	1408+1590
<b>C-H in plane bend</b>	1046+1216	1041+1216	1034+1081+1251
<b>C-S stretch</b>	835	835	833
<b>C-H out of plane bend</b>	707	718	710
<b>ring in plane deformation</b>	642	597	out of range

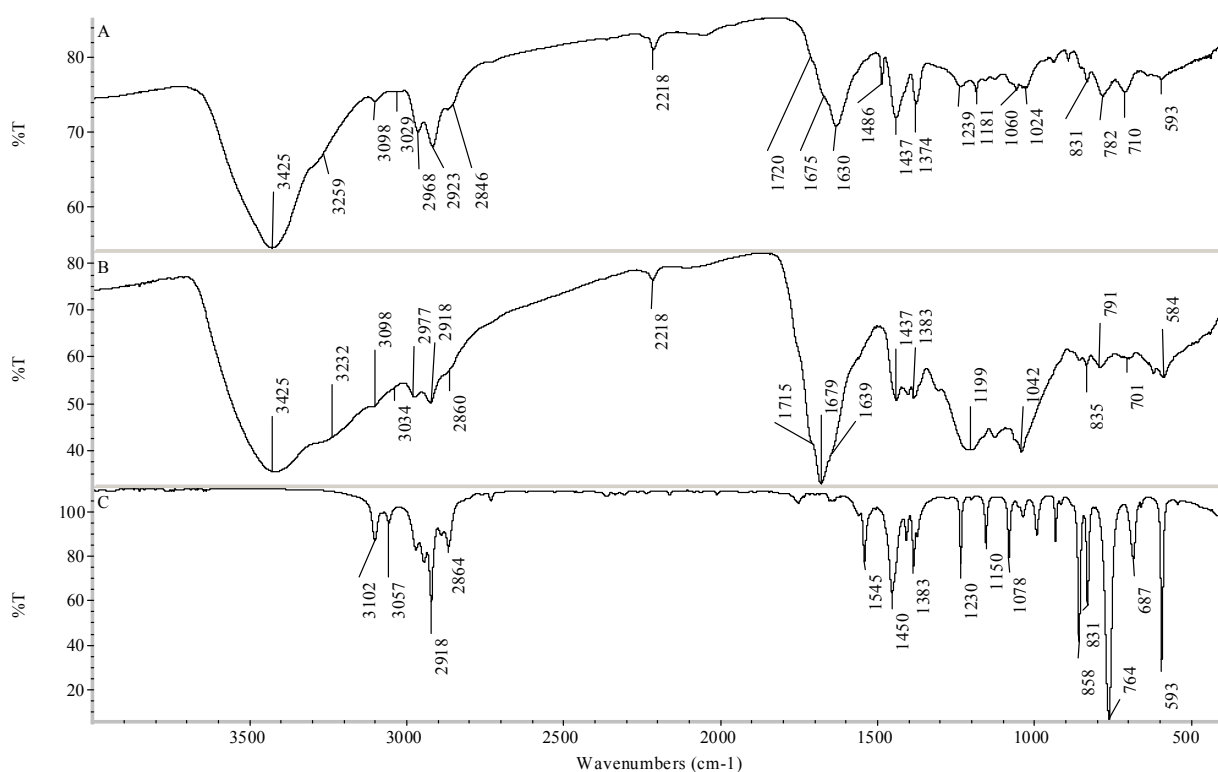


Figure 3: Infrared spectra of (A) poly(3-methylthiophene) plasma polymerized in nitrogen gas, (B) poly(3-methylthiophene) plasma polymerized in a nitrogen/oxygen mixture, (C) the monomer 3-methylthiophene.

Table 5: Detailed infrared peak assignment of (A) poly(3-methylthiophene) plasma polymerized in nitrogen (B) poly(3-methylthiophene) plasma polymerized in a nitrogen/oxygen mixture (c) the monomer 3-methylthiophene.

<b>Vibration</b>	<b>A (cm<sup>-1</sup>)</b>	<b>B (cm<sup>-1</sup>)</b>	<b>C (cm<sup>-1</sup>)</b>
<b>O-H</b> stretch	3425	3425	-
<b>C≡C-H</b> stretch	3259	3232	-
<b>C=C-H</b> stretch	3029+3098	3034+3098	3057+3102
<b>C-C-H</b> stretch	2846-2968	2860-2977	2864-2970
<b>C≡C</b> stretch	2218	2218	-
<b>C=O</b> stretch	1630+1675+1720	1639+1679+1715	-
<b>C=C</b> stretch	1437+1486	1437	1545
<b>C-H</b> deformations	850-1450	850-1450	850-1450
<b>C-S</b> stretch	831	835	831
<b>C-H</b> out of plane bend	710+782	701+791	687+764
<b>ring</b> in plane deformation	593	584	593

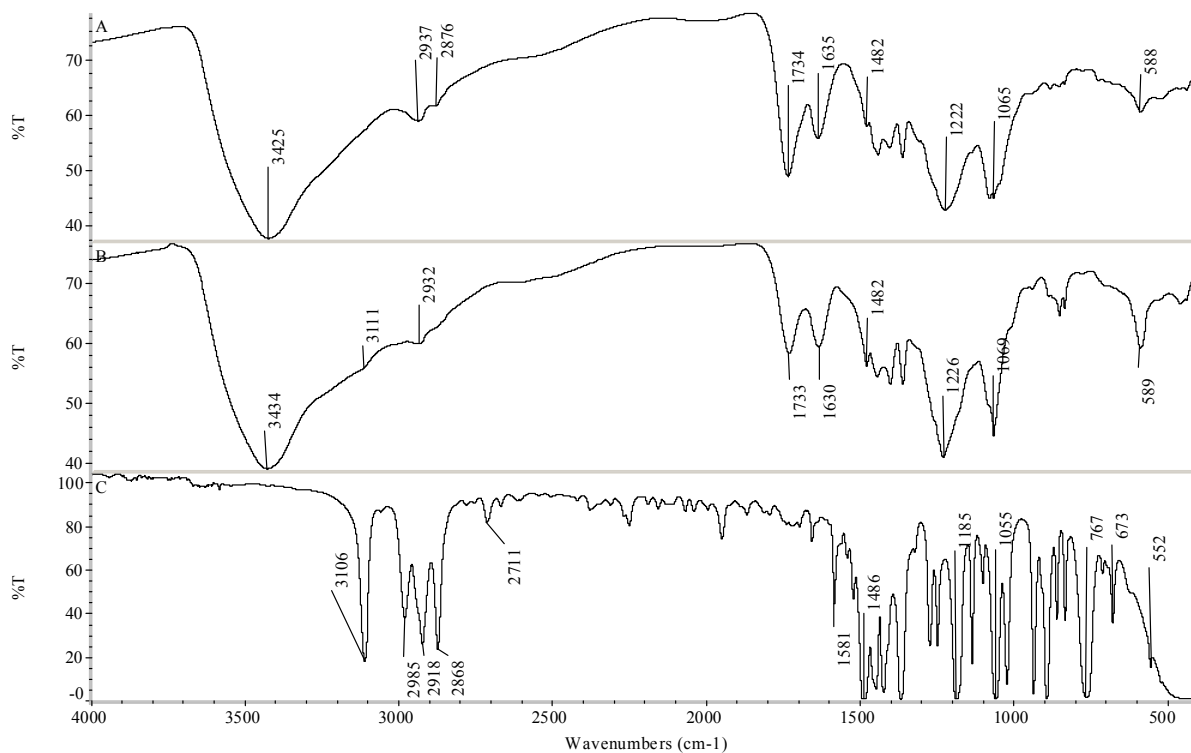


Figure 4: : Infrared spectra of (A) polyEDOT plasma polymerized at 5 cm from the gas inlet, (B) polyEDOT plasma polymerized at 10 cm from the gas inlet, (C) the monomer EDOT.

Table 6: Detailed infrared peak assignment of (A) polyEDOT plasma polymerized at 5 cm from the gas inlet, (B) polyEDOT plasma polymerized at 10 cm from the gas inlet, (C) the monomer EDOT.

Vibration	A (cm <sup>-1</sup> )	B (cm <sup>-1</sup> )	C (cm <sup>-1</sup> )
<b>O-H</b> stretch	3425	3434	-
<b>C=C-H</b> stretch	-	3111	3106
<b>C-C-H</b> stretch	2876-2937	2932	2868-2985
<b>C=O</b> stretch	1635+1734	1630+1733	-
<b>C=C</b> stretch	1482	1482	1486+1581



<b>C-H</b> deformations	850-1500	850-1500	850-1500
<b>C-O</b> stretch	1065+1222	1069+1226	1055+1185
<b>C-H</b> out of plane bend	-	-	673+767
<b>ring</b> in plane deformation	588	589	552

---

FT-IR spectra of the coatings polymerized from 3-methylthiophene, as well as the monomer spectrum are presented in figure 3. A detailed peak assignment is presented in table 5. The results with this monomer are similar to those with thiophene. Again, the aromatic ring structure is found in the plasma deposited coating (bands around  $1440\text{ cm}^{-1}$  and  $600\text{ cm}^{-1}$ ), as well as the double bonds ( $3030\text{ cm}^{-1}$  - not very clear due to overlap with the water O-H stretching band). C-H stretching at  $3100\text{ cm}^{-1}$ , is an indication of low molecular weight and non conventional cross linking. Some evidence for fragmentation is also seen. Terminal alkyne ( $3300\text{ cm}^{-1}$ ,  $2200\text{ cm}^{-1}$ ) and ketone functions (around  $1650\text{ cm}^{-1}$ ) are formed. The infrared spectra of the polymers plasma polymerized in nitrogen and a nitrogen/oxygen mixture, are very similar. Although a difference might be seen when looking at the carbonyl peaks. Besides the higher intensity of the carbonyl peaks, when oxygen is used, there is also a difference in the ratio between the different ketone functions. There are almost no saturated ketones (around  $1715\text{ cm}^{-1}$ ) present in the coating when the plasma contains only nitrogen. The number of saturated ketones increases when oxygen is added to the plasma carrier gas, which is an indication for a decrease in conjugation length. This might again be explained by the higher breakdown of double bonds by ozone and radical oxygen, when oxygen is present in the plasma carrier gas.

Figure 4 presents the FT-IR spectra of the coatings polymerized from EDOT, as well as the monomer spectrum. A detailed peak assignment is presented in table 6. A comparison is

made between the sample polymerized close to the gas inlet (A) and the one located at 10 cm from the gas inlet (B). Close to the gas inlet, the polyEDOT coating does not show the C-H stretch at  $3100\text{ cm}^{-1}$ , that can be found in the monomer spectrum (C). This means that most rings are substituted at the 2 and 5 position, as expected in a normal polymerization mechanism. Furthermore, there are no absorption peaks at  $2200\text{ cm}^{-1}$ , which means that alkyne functions are not present. Infrared absorption around  $1480\text{ cm}^{-1}$  (C=C stretch in ring) and  $590\text{ cm}^{-1}$  (ring in plane vibration) are indications that at least a part of the monomer ring structure is still present in the coating. However, there is still some fragmentation, which might be caused by the ozone and oxygen radicals, that originate from the oxygen added to the carrier gas. The ozone and oxygen radicals can break double bonds and lead to ketones (or aldehydes) and esters. The ketone can be clearly seen in the infrared spectrum around  $1630\text{ cm}^{-1}$ . Besides the infrared absorption of ketone functions, there's another carbonyl absorption present at  $1725\text{ cm}^{-1}$ . This peak is typical for ester functions, that can originate from the breaking of the double bond next to the six ring ether function of EDOT (figure 1c). Both the ketone and ester functions are  $\alpha,\beta$ -unsaturated. The sample that is polymerized at a distance of 10 cm from the gas inlet shows a similar spectrum (figure 4B). However some differences can be found. The shoulder at  $3100\text{ cm}^{-1}$  (C-H stretch on double bonds) shows that not all EDOT rings are substituted at the 2 and 5 positions. This is an indication for low molecular weight polymers. Another difference is found in the carbonyl absorptions. The ester carbonyl absorption at  $1725\text{ cm}^{-1}$  is not so strong as in the sample close to the gas inlet. This is an indication that there is less fragmentation further away from the gas inlet. These results confirm the reaction mechanism that was stated earlier. During the plasma on time, coating is only formed close to the gas inlet. Degree of fragmentation is then high in the highly reactive plasma. When the plasma power is turned off, reaction occurs at the

complete electrode surface. At this point, the more gentle conditions lead to less fragmentation.

In conclusion can be stated that fragmentation during plasma deposition at atmospheric pressure of polyEDOT, can be reduced by pulsing. However, the presence of carbonyl compounds still indicates some structural defects. Plasma deposition of polythiophene and poly(3-methylthiophene) leads to many defects such as unintended cross linking and degradation of the monomer structure with the formation of carbonyl and alkyne functions.

## **2.4. Optical Properties**

Conjugated polymers absorb light in the visual range, which gives them their typical color. This absorption behavior can be studied with UV/VIS spectroscopy. Figure 5 shows the absorption spectra of plasma polymerized polythiophene and poly(3-methylthiophene). Both polymers display a red color when polymerized traditionally. An absorption maximum around 400-500 nm is expected. However the plasma polymers all show a yellow-brown color. Figure 5 shows no absorption maximum between 400 and 500 nm, but a broad absorption close to the UV region. This means that the conjugation length in the plasma polymers is very short. The absorption band close to the UV region is expected to be the result of substitutions onto the thiophene rings and of short elongations of the conjugated system.

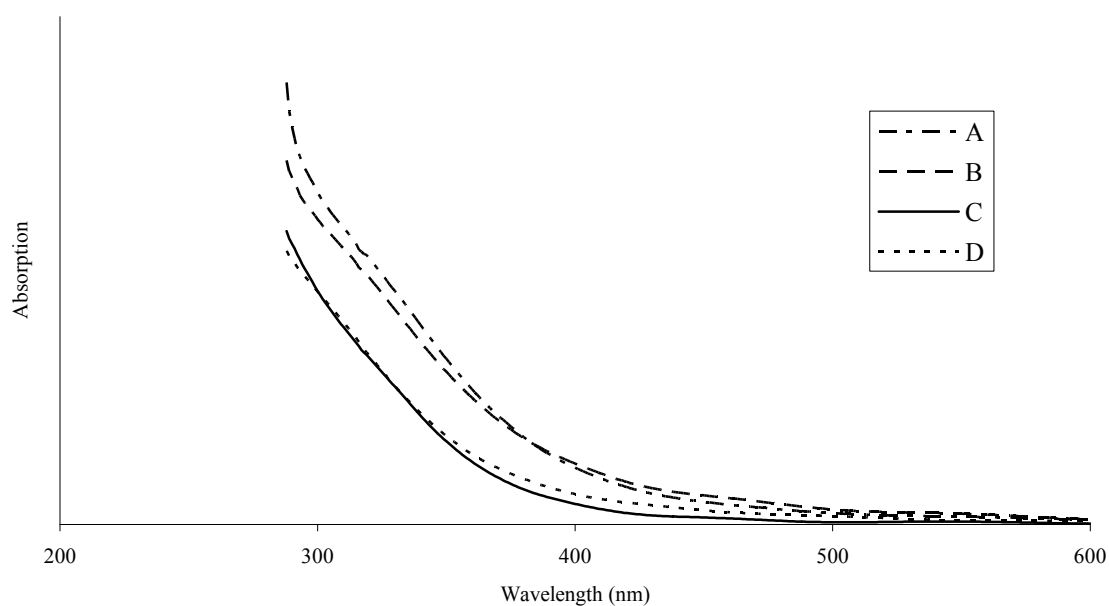


Figure 5: UV/VIS spectra of plasma polymerized polythiophene and poly(3-methylthiophene), deposited in two different carrier gasses: (A) polythiophene from a nitrogen plasma; (B) polythiophene from a nitrogen/oxygen plasma; (C) poly(3-methylthiophene) from a nitrogen plasma; (D) poly(3-methylthiophene) from a nitrogen/oxygen plasma.

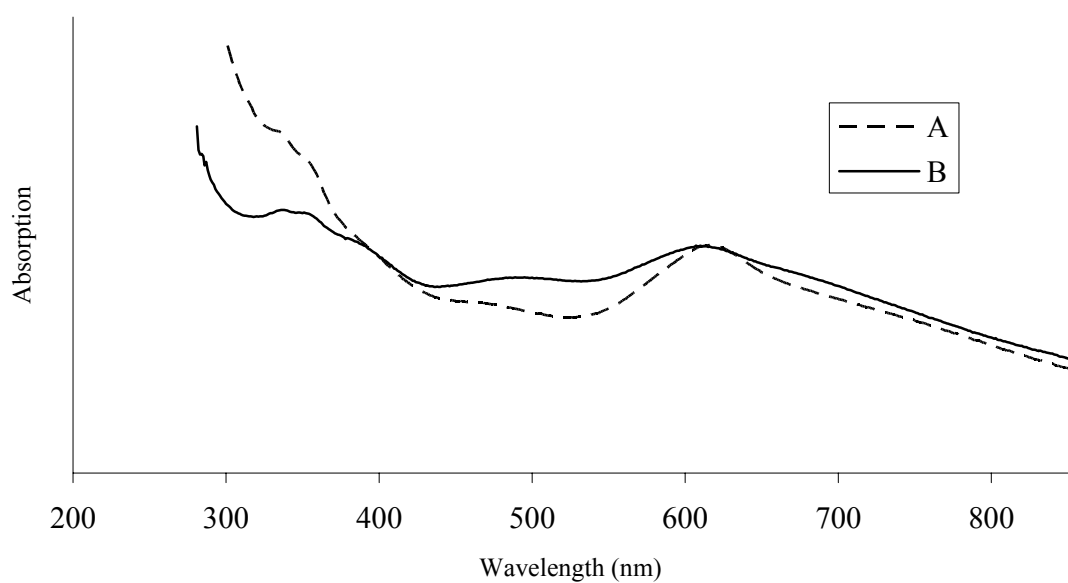


Figure 6: UV/VIS spectra of plasma polymerized poly(3,4-ethylenedioxythiophene) deposited at two different distances from the gas inlet: (A) 5 cm; (B) 10 cm.

The absorption spectra of the plasma polymerized polyEDOT are shown in figure 6. When the sample is deposited at a distance of 10 cm from the gas inlet (figure 6B), the coating has a bleu color; which is also the color of traditionally synthesized polyEDOT. The absorption spectrum of the plasma polymer shows an absorption maximum at 600 nm which is the expected value for undoped polyEDOT. There's also an absorption band around 350 nm. This band is due to parts of the polymer that consists of smaller conjugation lengths. After all, as was already discussed in the former chapter, the polyEDOT is still partially fragmented. The plasma polyEDOT, deposited close to the gas inlet has a green-bleu color. Figure 6A shows that this sample has the same absorption bands as the sample that was deposited at a 10 cm distance from the gas inlet. However, the ratio of the absorption maxima at 350 to 600 nm, is larger, when the polymer is deposited close to the gas inlet. This means that there is more fragmentation and less conjugation in this case, which again confirms the results of the former chapter.

In conclusion can be stated that plasma depositions at atmospheric pressure of polyEDOT coatings show an absorption spectrum that is resembling the typical spectrum for these kind of polymers. This is an indication that an elongated conjugated system is formed during pulsed plasma deposition. Probably, it is formed during the off times.

## **2.5. Conductivity**

Conjugated polymers can be turned into conducting polymers after doping. In this article, iodine vapour is used as a doping agent. The conductivity of the samples is determined by

measuring the resistance under normal circumstances (see experimental part), immediately after doping. The conductivity before and after doping is shown in table 7.

Table 7. Conductivity of plasma polymerized thiophene derivatives

N°	Monomer	Oxygen <sup>[a]</sup>	Position <sup>[b]</sup> (cm)	Conductivity <sup>[c]</sup> (undoped) (S/cm)	Conductivity <sup>[c]</sup> (doped) (S/cm)
<b>1</b>	<b>Th</b>	-	<b>5</b>	$< 1 \times 10^{-5}$	$1,1 \times 10^{-4}$
<b>2</b>	<b>Th</b>	+	<b>5</b>	$< 1 \times 10^{-5}$	$1,3 \times 10^{-5}$
<b>3</b>	<b>3MeTh</b>	-	<b>5</b>	$< 1 \times 10^{-5}$	$< 1 \times 10^{-5}$
<b>4</b>	<b>3MeTh</b>	+	<b>5</b>	$< 1 \times 10^{-5}$	$< 1 \times 10^{-5}$
<b>5a</b>	<b>EDOT</b>	+	<b>5</b>	$2,8 \times 10^{-4}$	$5,4 \times 10^{-4}$
<b>5b</b>	<b>EDOT</b>	+	<b>10</b>	$1,0 \times 10^{-2}$	$1,8 \times 10^{-3}$

[a] (+) Oxygen is present in the carrier gas; (-) No oxygen in the carrier gas.

[b] The position of the sample on the electrode is presented as the distance from the gas inlet.

[c] Conductivities smaller than  $1 \times 10^{-5}$  S/cm could not be measured with the equipment used.

Without doping, the plasma deposited polythiophene (1-2) and poly(3-methylthiophene) (3-4) coatings act as an insulator. After doping with iodine vapour, the poly(3-methylthiophene) coating still does not show any (semi)conductive properties. High degree of fragmentation results in short conjugation lengths and bad conductive properties. The polythiophene coatings show better results after doping with iodine vapour. Conductivities in the range of  $10^{-4}$  to  $10^{-5}$  S/cm can be measured. When deposition occurs in a pure nitrogen plasma, conductivity is one order of magnitude higher. Addition of oxygen to the plasma results in the formation of ozone and oxygen radicals, which are able to break up

double bonds. Breaking of double bonds causes a decrease in conjugation length, which leads to a decrease in conductivity. Although plasma depositions of polythiophene show some (semi)conductive properties, the degree of fragmentation is still high and results are not good. The low conductivity that is measured, might be caused by ion conductivity. Better results can be obtained by using the EDOT monomer.

PolyEDOT coatings are easily oxidized and are very stable in their oxidized state. For this reason they are already partially doped during the plasma reaction. Table 7 (5a-5b) shows that conductivities in the range of  $10^{-2}$  to  $10^{-4}$  can be measured without addition of any doping agent. Conductivity is two orders of magnitude higher for the sample deposited at a distance of 10 cm from the gas inlet. This result agrees well with the former hypothesis about fragmentation. Lower degree of fragmentation results in higher conductivity. To increase the conductivity of the plasma deposited polyEDOT, the coatings are doped in iodine vapour. The conductivity of the coating deposited close to the gas inlet, indeed increases. However, the coating that is deposited at 10 cm from the gas inlet, shows a decrease in conductivity. It is so far unclear why additional doping causes an actual decrease in conductivity. It may be possible that remaining radicals elongate the conjugated system and so are partially responsible for the measured conductivity. Doping may then cause a partial degradation of that conjugated system.

In conclusion can be stated that polyEDOT coatings, deposited in a plasma at atmospheric pressure have (semi)conductive properties. A conductivity of  $1 \times 10^{-2}$  S/cm can be reached without dopant addition.

### **3. Conclusions**

Plasma deposition at atmospheric pressure of polythiophene and poly(3-methylthiophene) leads to many structural defects. High reactivity of the plasma and formation of ozone and

oxygen radicals causes fragmentation with formation of carbonyl compounds and alkyne functions. The resulting coatings are highly cross linked. Although conductivities up to  $1 \times 10^{-4}$  S/cm can be reached by plasma depositing polythiophene, it seems that no conjugated polymer is formed. The measured conductivity might be due to ion conductivity. Better results are accomplished with the deposition of polyEDOT. By using a pulsed plasma, structural defects can be reduced. The plasma deposited polyEDOT has a blue colour and an absorption band around 600 nm, which are clear indications of an elongated conjugated system. Conductivities up to  $1 \times 10^{-2}$  S/cm can be reached without the use of a doping agent. It is so far unclear why doping causes a decrease in conductivity. Possibly, remaining radicals cause a degradation of the conjugated system.

## **4. Experimental Part**

### **4.1. Materials**

The monomers used in this article are thiophene (99+%), 3-methylthiophene (98%) and 3,4-ethylenedioxythiophene. All monomers were purchased from Sigma Aldrich and were used as received. The dopant iodine (99.8%, ACS reagent) was also purchased from Sigma Aldrich and used without further purification.

### **4.2. Plasma Deposition**

A schematic figure of the plasma reactor is depicted in figure 7. The plasma is generated with a dielectric barrier discharge between two horizontally placed electrodes. The lower electrode (A) is covered by a glass dielectric (B) of 5 mm thickness, while the upper electrode (C) is uncovered. A high ac voltage is used on the lower electrode. Power is supplied by an ENI DC power supply. With a MELEC switching unit the DC voltage is turned over in an ac voltage before it is transformed up to high voltage. By carefully tuning



the on and off times (dead time) of the switching unit, power losses can be minimized. However it is difficult to measure power losses in a filamentary discharge, the power loss is estimated to be 10 to 20%. The upper electrode is grounded. The gap (D) between the glass dielectric and the uncovered electrode is 1,5 mm. All reactions occurred at a fixed frequency of 1,5 kHz. The precursor was injected into the plasma as an aerosol, generated with an atomizer (E) at a 2 bar nitrogen pressure. The atomizer used, is a TSI constant output atomizer. Compressed gas is expanded through an orifice to form a high velocity jet. Liquid is drawn into the atomizing section through a vertical passage and is then atomized by the jet. By impact with the wall, opposite to the jet, large droplets are removed. The removed liquid is recirculated. With this system it is possible to create high aerosol concentrations ( $2 \times 10^6$  particles/cm<sup>3</sup>) with droplet diameters around 0.3  $\mu$ m. Before entering the plasma the aerosol is mixed with the carrier gas. The gas flow was adjusted with a mass flow controller (F). The coatings were deposited onto glass substrates which were placed onto the dielectric. Before deposition, the glass substrates were carefully cleaned with isopropyl alcohol in an ultrasonic bath.

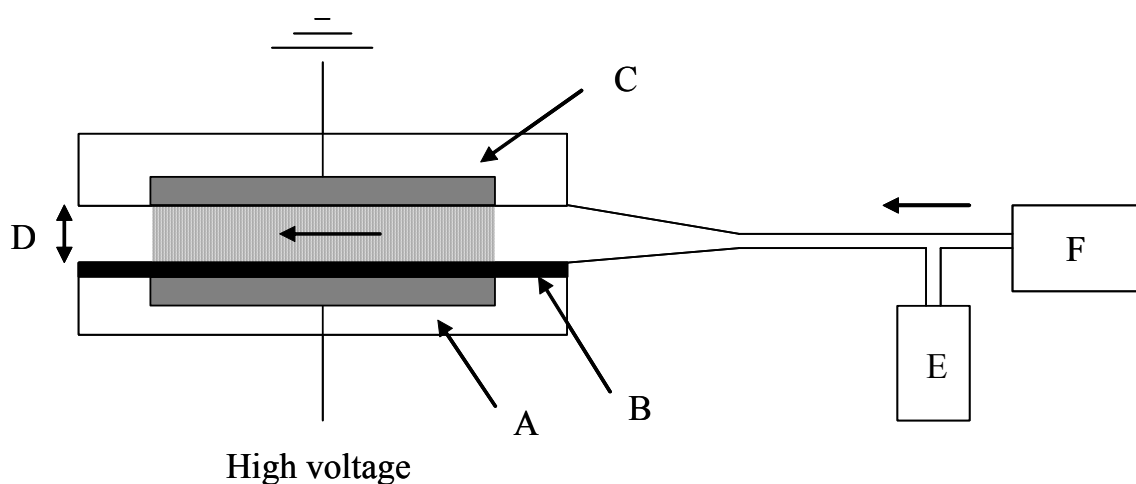


Figure 7: A plasma reactor, containing: (A) a high voltage electrode, (B) a glass dielectric, (C) a grounded electrode, (D) an inter electrode gap, (E) an atomizer containing precursor, (F) a mass flow controller which controls the carrier gas flow.

### 4.3. Analytical Techniques

The thickness of the plasma deposited coatings was measured with an UBM profilometer.

The composition of the plasma deposited coatings was studied with an x-ray photoelectron spectrometer (XPS) from Thermo with a theta probe.

The chemical structure of the plasma deposited coatings was studied with a Nexus Fourier transformed infrared spectrometer from Thermo. The samples were measured after scraping off the coating from the glass substrate and mixing it with potassium bromide. This mixture was pressed into a pellet with a pressure of 8 ton. The potassium bromide (99+, FTIR grade) was purchased from Sigma Aldrich and used after drying at 120°C. Spectra were obtained after measuring the %transmittance through the pellet and after subtraction of the nitrogen background. Analysis of the spectra was done with help of the book edited by D.H. Williams and I. Fleming<sup>[28]</sup>

The absorption of UV and visual light by the plasma deposited coatings was measured with a Lambda 900 UV/VIS/NIR spectrometer from Perkin Elmer.

The conductivity of the plasma deposited coatings was calculated from their resistance. First, two silver electrodes were coated onto the coating surface with silver paste. After drying, the coating was brought into a chamber with a constant humidity of 50% at 25°C. The resistance of the coating was measured with a Fluke 189 True RMS multimeter. Specific conductivity was calculated from these resistance measurements.

- [1] H. Shirakawa, E. J. Louis, A. G. MacDiarmid, A. J. Heeger, Chem. Commun. **1977**, 578
- [2] A. Dodabalapur, Solid State Communications **1997**, 102, 259
- [3] R. E. Martin, F. Geneste, A. B. Holmes, Comptes Rendus de l' Académie des Sciences - Series IV - Physics **2000**, 1, 447
- [4] V. Saxena, B. D. Malhotra, Current Applied Physics **2003**, 3, 293
- [5] D. Natali, M. Sampietro, Nuclear Instruments and Methods in Physics Research Section A **2003**, 512, 419
- [6] B. Adhikari, S. Majumdar, Progress in Polymer Science **2004**, 29, 699
- [7] J.-M. Nunzi, Comptes Rendus Physique **2002**, 3, 523
- [8] P. Zarras, N. Anderson, C. Webber, D. J. Irvin, J. A. Irvin, A. Guenther, J. D. Stenger-Smith, Radiation Physics and Chemistry **2003**, 68, 387
- [9] A. Pron, P. Rannou, Progress in Polymer Science **2002**, 27, 135
- [10] K. Gurunathan, A. V. Murugan, R. Marimuthu, U. P. Mulik, D. P. Amalnerkar, Materials Chemistry and Physics **1999**, 61, 173
- [11] D. H. Shin, S. D. Lee, K. P. Lee, S. Y. Park, D. H. Choi, N. Kim, Synthetic Metals **1995**, 71, 2263
- [12] M. S. Silverstein, I. Visoly-Fisher, Polymer **2002**, 43, 11
- [13] M. C. Kim, S. H. Cho, J. G. Han, B. Y. Hong, Y. J. Kim, S. H. Yang, J. H. Boo, Surface & Coatings Technology **2003**, 169, 595
- [14] J. Wang, K. G. Neoh, E. T. Kang, Thin Solid Films **2004**, 446, 205
- [15] Y.-J. Yu, J.-G. Kim, J.-H. Boo, Journal of Materials Science Letters **2002**, 21, 951
- [16] L. M. H. Groenewoud, G. H. M. Engbers, J. Feijen, Langmuir **2003**, 19, 1368

- [17] L. M. Groenewoud, A. E. Weinbeck, G. H. Engbers, J. Feijen, *Synthetic Metals* **2002**, 126, 143
- [18] M.-C. Kim, S.-H. Cho, S.-B. Lee, Y. Kim, J.-H. Boo, *Thin Solid Films* **2004**, 447, 592
- [19] A. Kiesow, A. Heilmann, *Thin Solid Films* **1999**, 343-344, 338
- [20] K. Tanaka, K. Yoshizawa, T. Takeuchi, T. Yamabe, J. Yamauchi, *Synthetic Metals* **1990**, 38, 107
- [21] B. Thomas, M. G. K. Pillai, S. Jayalekshmi, *Journal of Physics D: Applied Physics* **1988**, 21, 503
- [22] N. V. Bhat, D. S. Wavhal, *Journal of Applied Polymer Science* **1998**, 70, 203
- [23] N. V. Bhat, D. S. Wavhal, *Separation Science and Technology* **2000**, 35, 227
- [24] L. M. H. Groenewoud, G. H. M. Engbers, J. G. A. Terlingen, H. Wormeester, J. Feijen, *Langmuir* **2000**, 16, 6278
- [25] Z. J. Horvath, *Journal of Applied Physics* **1990**, 68, 5899
- [26] Z. S. Tong, T. S. Pu, M. Z. Wu, Z. Y. Zhang, J. Zhang, R. P. Jin, D. Z. Zhu, D. X. Cao, F. Y. Zhu, J. Q. Cao, *Synthetic Metals* **1996**, 79, 85
- [27] L. M. H. Groenewoud, G. H. M. Engbers, R. White, J. Feijen, *Synthetic Metals* **2001**, 125, 429
- [28] *Spectroscopic methods in organic chemistry, fourth edition* (Eds: D.H Williams, I. Fleming, McGraw-Hill book company, London **1989**).